

Pressure and temperature dependences of the elastic constants of compression-annealed pyrolytic graphite

W. B. Gauster and I. J. Fritz

Citation: *Journal of Applied Physics* **45**, 3309 (1974); doi: 10.1063/1.1663777

View online: <http://dx.doi.org/10.1063/1.1663777>

View Table of Contents: <http://scitation.aip.org/content/aip/journal/jap/45/8?ver=pdfcov>

Published by the [AIP Publishing](#)

Articles you may be interested in

[Erratum: Pressure and temperature dependences of the elastic constants of compression-annealed pyrolytic graphite](#)

J. Appl. Phys. **46**, 3697 (1975); 10.1063/1.322285

[Elastic Constants and Electron-Microscope Observations of Neutron-Irradiated Compression-Annealed Pyrolytic and Single-Crystal Graphite](#)

J. Appl. Phys. **41**, 3389 (1970); 10.1063/1.1659430

[Elastic Constants of Compression-Annealed Pyrolytic Graphite](#)

J. Appl. Phys. **41**, 3373 (1970); 10.1063/1.1659428

[Expansion of Annealed Pyrolytic Graphite](#)

J. Appl. Phys. **35**, 1992 (1964); 10.1063/1.1713794

[Compressibility of Pyrolytic Graphite](#)

J. Chem. Phys. **40**, 71 (1964); 10.1063/1.1724896

The image shows the cover of an AIP Applied Physics Reviews journal. It features a blue and orange color scheme with a molecular structure graphic. The text 'AIP Applied Physics Reviews' is at the top left. The main title 'NEW Special Topic Sections' is in large white letters. Below it, 'NOW ONLINE' is in orange, followed by 'Lithium Niobate Properties and Applications: Reviews of Emerging Trends' in white. The AIP logo and 'Applied Physics Reviews' are at the bottom right.

NEW Special Topic Sections

NOW ONLINE
Lithium Niobate Properties and Applications:
Reviews of Emerging Trends

AIP Applied Physics Reviews

Pressure and temperature dependences of the elastic constants of compression-annealed pyrolytic graphite*

W. B. Gauster and I. J. Fritz

Sandia Laboratories, Albuquerque, New Mexico 87115
(Received 4 February 1974)

Changes of ultrasonic transit times in compression-annealed pyrolytic graphite (CAPG) were measured as a function of temperature (4–300 °K at atmospheric pressure) and of pressure (0–20 kbar at 295 °K). From the low-temperature results, obtained for five independent acoustic modes, the temperature variations of all five elastic constants were calculated using the thermal expansion data of Bailey and Yates. From the high-pressure data, taken for four independent modes, the changes of all five elastic constants and of the unit cell dimensions with pressure were calculated under the assumption that the small a -axis compressibility is independent of pressure. The initial pressure derivatives of C_{33} and C_{44} are, respectively, about 25 and 35% lower than those obtained by Green *et al.* for CAPG. The pressure dependences of the volume and c -axis compressibilities are in good agreement with measurements on natural graphite crystals by Lynch and Drickamer and by Bridgman, and in less satisfactory agreement with data of Kabalkina and Vereshchagin. The results support the contention that CAPG has bulk elastic properties very similar to those of single-crystalline graphite.

I. INTRODUCTION

A number of the interesting properties of crystalline graphite are attributable to the material's extreme anisotropy. This characteristic is evident from the interatomic spacings of about 1.4 Å within the basal planes and about 3.4 Å between them, and the corresponding bond energies of about 5 eV versus less than 0.2 eV.¹ The unusual structure of graphite leads to a broad range of properties in carbon materials, which is being utilized in the development of carbon-carbon composites for a variety of applications.² The resulting materials are extremely complex to characterize. Even for one of the most readily characterized carbons, single-crystal graphite, there is a scarcity of data on basic elastic properties. Natural graphite crystals typically have a layer diameter of only a few millimeters, and ultrasonic techniques have not been used to measure their elastic properties.

The development of compression-annealed pyrolytic graphite (CAPG), however, has provided a material whose structure closely approximates that of a single crystal and which can be prepared in sufficiently large sizes to permit use of standard testing techniques. The properties of CAPG are the subject of this paper. Using ultrasonic through-transmission and pulse-superposition techniques, measurements were made of acoustic delays at room temperature from 0 to 20 kbar and at atmospheric pressure from 4 to 300 °K. Using thermal expansion values from the literature in the case of the low-temperature data, and calculating compressibilities iteratively from the high-pressure data, sets of elastic constants were obtained as a function of temperature and pressure.

II. MATERIAL PREPARATION AND PREVIOUS MEASUREMENTS OF ELASTIC CONSTANTS

The basic procedure of preparing CAPG was described by Ubbelohde, Young, and Moore.³ Disks of pyrolytic graphite are compressed uniaxially along the c axis to a maximum of 4000–5000 psi (275–345 bar) at a temperature of 2800–3000 °C. The final CAPG material has a density of 2.26 g/cm³, while the single-crystal value is

2.266 or 2.267 g/cm³. The layer diameters are 20–50 μ and the alignment of c axes is to within a few tenths of a degree. Interlayer spacings are 3.355–3.357 Å, compared to a single-crystal value of 3.354 Å. The a axes are still randomly oriented, but since acoustic wave propagation is isotropic in the basal plane of a hexagonal crystal, the CAPG displays the same symmetry for ultrasonic measurements as the crystal, whose structure it closely approximates.

Elastic constants of CAPG have been determined by Blakslee *et al.* at ambient temperature and pressure in an extensive series of experiments involving ultrasonic, resonance, and static tests.⁴ The results are listed in Table I. The constants are believed to approach closely those of a single crystal, and there is good agreement with certain values for natural graphites calculated, for example, from specific heat and compressibility (see Ref. 4 for a chronological listing). A comment is required on the value of C_{44} . Because of the high density and mobility of dislocations in the basal plane, the value in Table I is expected to be low compared to the intrinsic C_{44} of a single crystal. This was substantiated by elastic constant measurements on CAPG as a function of neutron irradiation by Seldin and Nezbeda,⁵ who found no changes in the constants except for C_{44} , which reached a limiting value of 0.40×10^{11} dyn/cm² (more than an order of magnitude greater than before irradiation) at a dose of 7.1×10^{18} nvt at 50 °C. The increase in C_{44} is attributed to the pinning of dislocations, and the higher value more nearly represents the intrinsic basal plane shear constant of graphite.

The present experiments involved relative measurements; the changes of acoustic delay with temperature and pressure were determined. Where numerical values of the constants are given, they were calculated using the values of Ref. 4 as a base. For C_{44} , a mean value

TABLE I. Room-temperature atmospheric pressure elastic constants of compression-annealed pyrolytic graphite, in units of 10^{11} dyn/cm² (Ref. 4).

C_{33}	C_{44}	C_{11}	C_{12}	C_{13}
3.65 ± 0.10	$0.018-0.035$	106 ± 2	18 ± 2	1.5 ± 0.5

TABLE II. Modes of acoustic propagation and effective elastic constants for hexagonal symmetry. Notation for columns 2 and 3: c , parallel to c axis; a , perpendicular to c axis.

Mode	Propagation direction	Polarization direction	ρv^2
1	c	c (longitudinal)	C_{33}
2	c	a (transverse)	C_{44}
3	a	a (longitudinal)	C_{11}
4	a	a (transverse)	$\frac{1}{2}(C_{11} - C_{12})$
5	a	c (transverse)	C_{44}
6	45° from c	a (transverse)	$\frac{1}{4}(C_{11} - C_{12} + 2C_{44})$
7	45° from c	45° from c (quasilongitudinal)	$\frac{1}{4}[C_{11} + C_{33} + 2C_{44} + [(C_{11} - C_{33})^2 + 4(C_{13} + C_{44})^2]^{1/2}]$
8	45° from c	$\perp a$ (quasitransverse)	$\frac{1}{4}[C_{11} + C_{33} + 2C_{44} - [(C_{11} - C_{33})^2 + 4(C_{13} + C_{44})^2]^{1/2}]$

of 0.028×10^{11} dyn/cm² was arbitrarily chosen. As will be seen below, no anomalous change in C_{44} due to "freezing" of dislocations was observed down to 1.75°K, suggesting a very small activation energy for dislocation motion.

III. EXPERIMENTAL METHODS

A. Sample preparation

The CAPG was available in sample sizes of several cm in the basal plane direction by a maximum of about 0.6 cm in the c direction. One of the principal experimental difficulties occurs in the normally simple procedures of handling and cutting the samples. Since the material delaminates easily parallel to the basal plane, cutting was done with a wire saw while clamping the specimens between pieces of unannealed graphite. To cut a sample with faces at 45° to the c axis, which was required to determine C_{13} directly, the sample was potted in a resin which was dissolved away after the cutting operation. Polishing faces parallel to the c direction or at 45° to it has to be done with extreme care. Fine sandpaper was used, followed by a piece of writing paper over a lapping plate. Faces parallel to the planes, however, are prepared easily—simply by stripping with adhesive tape.

B. Acoustic propagation modes

Table II lists the propagation and polarization directions for the modes used in the present experiments. Pressure runs were carried out for modes 1–4; the variation of C_{13} was calculated on the basis of some assumptions discussed below. Temperature runs were made on modes 1–4 and 8, and the variations of all five constants were calculated from the data.

C. Pressure runs

A standard Bridgman press with a 50–50 pentane-isopentane mixture as the pressure fluid was used to generate hydrostatic pressures up to 20 kbar. The pressure was monitored using a manganin wire coil that had been calibrated against the Bi I-Bi II phase transition. For the ultrasonic measurements, X-, Y-, and AC-cut quartz transducers, of $\frac{1}{8}$ -in.-diam active area, were bonded to the samples using either a phthalic anhydride-glycerin polymer or Nonaq stopcock grease.⁶ A pulse-superposition technique⁷ was used for modes 1, 3, and 4. For mode 2 (C_{44}), however, the echo train was of in-

sufficient quality for superposition, and the delay between applied and transmitted pulses was measured instead. The poorer quality of the signal was probably due to the higher attenuation in this mode than in others.

Obtaining a consistent set of data for all modes is tedious because of the properties of the sample material. One difficulty is that of preparing a smooth surface perpendicular to the basal planes, as discussed above. This accounts for part of the problem of obtaining a good bond between sample and transducer; often several attempts were required before a suitable signal was obtained. A further difficulty was due to delamination of the sample at high pressures. Several runs were terminated because of sample separation; in particular, this phenomenon accounted for the lack of success in determining C_{13} as a function of pressure from modes 7 or 8. Despite the careful preparation procedure, samples cut at 45° to the c axis delaminated in the pressure cell in the half-dozen attempts made. It was, however, possible to make low-temperature measurements for this orientation, which will be discussed below.

Both the phthalic anhydride-glycerin polymer and Nonaq stopcock grease were used as bonds because in some cases one appeared to give a better bond than the other. In general, signals were propagated more easily in the basal planes than perpendicular to them, although

TABLE III. Modes of acoustic propagation that provided the data used to determine the pressure dependence of the elastic constants of compression-annealed pyrolytic graphite.

Mode	Elastic constant	Frequency (MHz)	Transducer	Technique
1	C_{33}	5	X cut, fundamental	superposition
		15	X cut, 3rd harmonic	superposition
2	C_{44}	5	Y cut, fundamental	transmission ^a
3	C_{11}	10	X cut, fundamental ^b	superposition
		5	X cut, fundamental ^c	superposition
4	$\frac{1}{2}(C_{11} - C_{12})$	10	AC cut, fundamental	superposition
		30	AC cut, 3rd harmonic	superposition

^a Separate runs made on two different samples.

^b Nonaq bond, all other measurements with phthalic anhydride-glycerin.

^c More scatter than for 10 MHz run, but same slope.

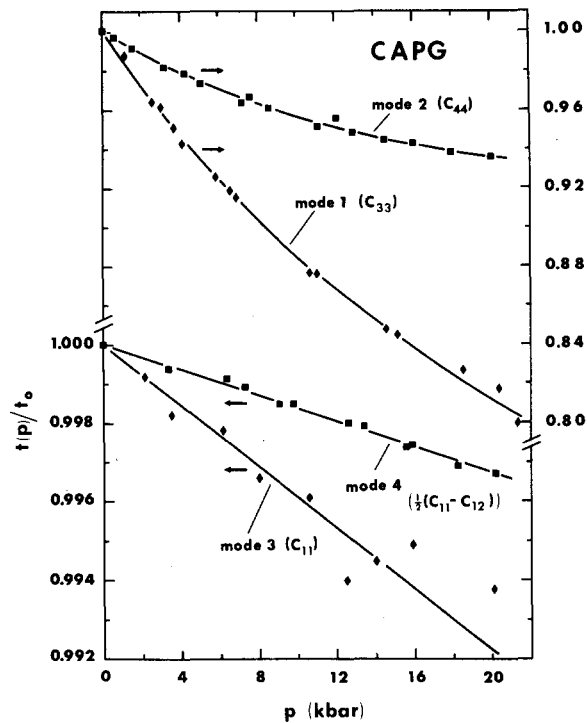


FIG. 1. Acoustic transit time $t(p)$ at pressure p divided by acoustic transit time t_0 at atmospheric pressure, for four propagation modes in compression-annealed pyrolytic graphite, plotted as a function of pressure p .

bonding of the transducers was more difficult for propagation in the planes. In some cases, the bond appeared to improve as pressure was applied, so that the decreasing pressure portion of the run yielded better results than the increasing part.

Table III is a listing of the combinations of transducers, bonds, and techniques that were used to obtain the pressure data from which the results were calculated.

D. Low temperature

The samples were situated in a variable-temperature liquid-helium cryostat, and measurements were taken at several intervals between room temperature and 4°K. For some runs, the temperature was lowered to 1.75°K by pumping on the liquid helium. 5-MHz X- and Y-cut quartz transducers, $\frac{1}{4}$ and $\frac{1}{8}$ in. in diameter, were used. Most measurements were made using two transducers and determining the delay with a calibrated delay pot on an oscilloscope, since it was not possible to obtain the very clean echo patterns required for superposition techniques.

A suitable bonding material over the entire temperature range was a rubber-base resin on transparent adhesive tape. The use of this material was first mentioned by Peters, Breazeale, and Paré.⁸ Both the sample and the transducer, the latter with a piece of tape over the surface to be bonded, are heated until the glue flows easily (about 150°C); then the tape is removed, leaving a layer of glue on the transducer. The transducer is attached to the sample, and the assembly is allowed to cool, preferably under some compression. To ascertain

that the bond did not introduce changes of acoustic delay as a function of temperature, several runs were made using silver-plated X-cut quartz samples, with transducers bonded in the same manner as to the graphite. No effect was observed.

Partial rechecking of the runs was done using higher acoustic frequencies, Nonaq stopcock grease bonds, and pulse-superposition measurements. Subsequent analysis indicated some possible problems with temperature gradients through the sample in the region between 200 and 270°K, and for some runs the intermediate temperature data are felt to be less certain than the high- and low-temperature points.

IV. RESULTS AND DATA ANALYSIS

A. Pressure

Figure 1 is a plot of the measured transit time as a function of pressure, divided by the transit time at atmospheric pressure, for the four modes listed in Table III. Note the differences in scales for the two pairs of modes. Much larger changes are seen for modes 1 and 2, whose propagation direction is along the easily compressed c axis, than for the modes propagating in the basal plane.

From these data, the variations of the elastic constants with pressure were calculated. This was done by a scheme similar to the one developed by Cook.⁹ The exact procedure used here was described recently by Fritz,¹⁰ who used it to analyze data on rutile. The general formula is

$$[C_{ij}(p)/C_{ij}(0)] = (\rho/\rho_0)(l/l_0)^2(f/f_0)^2, \quad (1)$$

where $C_{ij}(p)/C_{ij}(0)$ are the ratios of the elastic constants at pressure p to their values at atmospheric pressure. The terms ρ/ρ_0 , l/l_0 , and f/f_0 are, respectively, the ratios of mass density, sample length, and pulse repetition rate (reciprocal of transit time) at pressure p to their values at atmospheric pressure. For hexagonal symmetry, Eq. (1) can be expressed for modes 1 and 2 as

$$[C_{ij}(p)/C_{ij}(0)] = (f/f_0)^2(c/c_0)(a_0/a)^2, \quad (2)$$

and for modes 3 and 4 as

$$[C_{ij}(p)/C_{ij}(0)] = (f/f_0)^2(c_0/c), \quad (3)$$

where c/c_0 and a/a_0 are, respectively, the sample dimensions in the c direction and in the basal plane normalized to their values at atmospheric pressure. The measured changes of transit time (or repetition rate) are used to calculate both the changes of sample dimensions and of the elastic constants. First, the compressibilities in the two crystal directions are calculated from the atmospheric pressure values of the elastic constants. It is assumed that these compressibilities do not change over some small pressure interval—in our case 2 kbar. The changes in sample dimensions over the 2-kbar interval are calculated from the compressibilities, and the new sample dimensions and repetition rate data are used to evaluate the elastic constants at the higher pressure, using Eqs. (2) and (3).

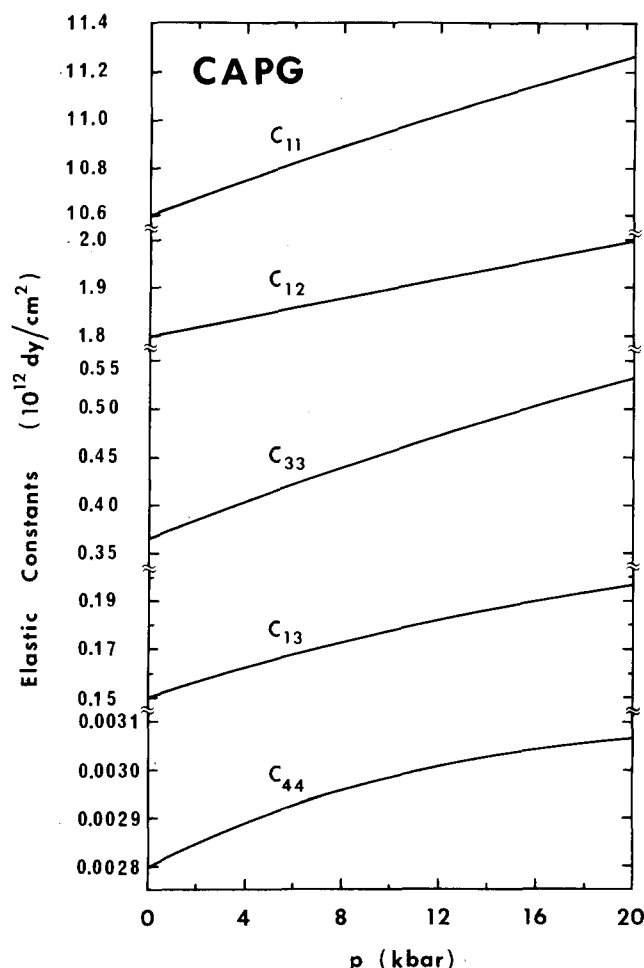


FIG. 2. Elastic constants of compression-annealed pyrolytic graphite as a function of pressure, calculated from the data of Fig. 1 and the atmospheric pressure elastic constants of Ref. 4.

The expressions for the compressibilities in terms of the elastic constants include C_{13} , which does not appear in the four measured mode velocities. Therefore, an additional assumption was introduced into the calculational scheme. The compressibility in the basal plane was assumed constant as a function of pressure, and C_{13} was determined from that compressibility and values of the other elastic constants. Since the compressibility in the basal plane is almost two orders of magnitude smaller than that in the c direction, the error introduced in the calculation of the constants other than C_{13} is less than the measurement error. The self-consistent procedure is continued over the entire pressure span. The errors due to ignoring the difference between adiabatic and isothermal compressibilities and using the coarse pressure net are negligible compared to the uncertainty in the data.

TABLE IV. Initial slopes of elastic constants with pressure at 295°K and with temperature at atmospheric pressure.

	C_{11}	C_{12}	C_{33}	C_{13}	C_{44}
$\left(\frac{\partial C}{\partial p}\right)_{T=295^\circ\text{K}}$	39	11	9.6	3.1	0.0023
$\left(\frac{\partial C}{\partial T}\right)_{p=1 \text{ bar}}^a$	11	2.6	0.46	8.0	0.10

^a Units of $10^9 \text{ dyn/cm}^2 \text{ } ^\circ\text{K}$.

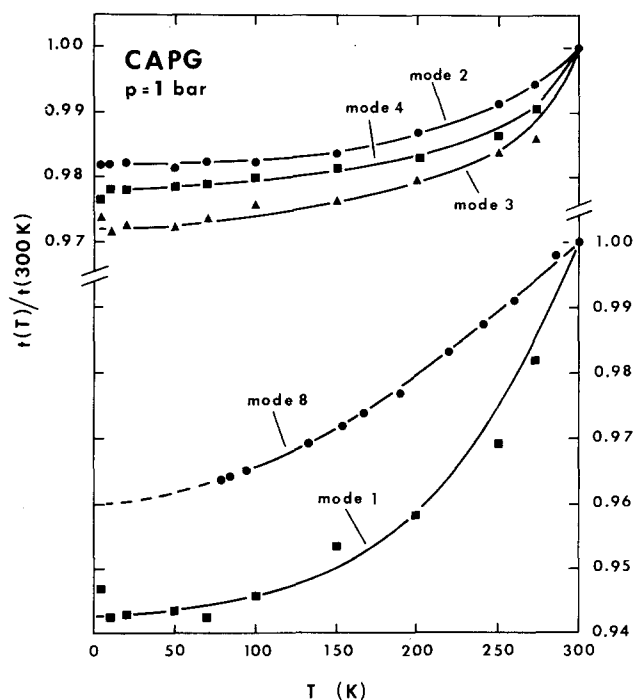


FIG. 3. Acoustic transit time $t(T)$ at temperature T divided by acoustic transit time t_0 at 300°K, for five propagation modes in compression-annealed pyrolytic graphite, plotted as a function of temperature T .

The final smoothed curves of the elastic constants as a function of pressure, calculated from the relative measurements as outlined above and from the atmospheric pressure elastic constants of Blakslee *et al.*,⁴ are shown in Fig. 2. An indication of the uncertainty in the final values is given by the run-to-run reproducibility, which is on the order of 10–15%. Measurements of sample lengths and of pulse repetition frequencies were accurate to fractions of 1%. Since the signals transmitted through the samples were usually of less than ideal shape, one of the main sources of error was the visual superposition of echoes on the oscilloscope (false resonances). The other principal uncertainty is the possible variation of properties from one sample to the next, due either to initial differences in crystallite alignment and structure or to the effects of cutting and polishing. The initial slopes ($\partial C/\partial p$) are listed in Table IV.

B. Temperature

Figure 3 is a plot of the ultrasonic data for five propagation modes. The transit times, normalized to their 300°K values, are plotted as a function of temperature. For modes 1, 3, and 4, the measurements were made down to 4°K; for mode 2 they were extended to 1.75°K; for mode 8 the run went only to 78°K and the data were extrapolated (dashed curve) below that temperature.

Figure 4 shows the smoothed values of the elastic constants as a function of temperature, calculated from the data of Fig. 3 and the room-temperature values of Table I. The thermal expansion values of Bailey and Yates¹¹ were used in the calculation. The experimental uncertainties are estimated to be on the same order as for the pressure runs, 10–15%, except for C_{13} , which is cal-

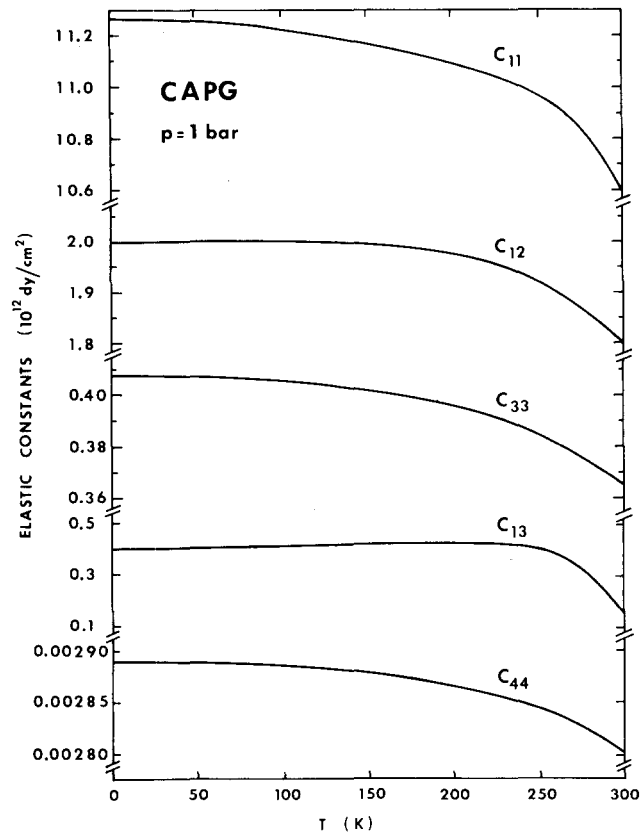


FIG. 4. Elastic constants of compression-annealed pyrolytic graphite as a function of temperature, calculated from the data of Fig. 3, room-temperature elastic constants of Ref. 4, and thermal expansion values of Ref. 11.

culated by taking the difference of large numbers. Since the signals for mode 8 were generally of a poorer quality than the others, the plot of C_{13} can only be regarded as a rough estimate. Of the remaining constants, the largest change is seen in C_{11} and the smallest in C_{44} . The small change in C_{44} suggests that the mobility of the dislocations accounting for the low value of C_{44} is so high that they could not be "frozen in". The initial slopes ($\partial C/\partial T$) are listed in Table IV.

V. DISCUSSION AND CONCLUSIONS

A. Temperature

There are no previous measurements with which to compare the low-temperature elastic constants of CAPG. It was noted above that no anomalous increase in C_{44} was observed between 300 and 1.75°K, suggesting that no freezing of dislocation motion occurred and that a very low activation energy is associated with their movement.

TABLE V. Grüneisen parameters parallel and perpendicular to the basal plane calculated from thermal expansion data of Ref. 11 and adjusted for temperature variation of elastic constants.

	270°K	50°K (Ref. 11)	50°K (Adjusted)
$\gamma_{ }$	0.69	3.29	3.42
γ_{\perp}	-0.84	-5.32	-3.42

In Ref. 11, Bailey and Yates calculated the Grüneisen parameters $\gamma_{||}$ and γ_{\perp} (parallel and perpendicular to the c axis, respectively) as a function of temperature, using their measured thermal expansion values in the expressions

$$\gamma_{||} = (V/C_t)(2C_{13}^s\alpha_{\perp} + C_{33}^s\alpha_{||}),$$

$$\gamma_{\perp} = (V/C_t)[(C_{11}^s + C_{12}^s)\alpha_{\perp} + C_{13}^s\alpha_{||}]. \quad (4)$$

Here C_t is the heat capacity at constant stress, V is the specific volume, C_{ij}^s are the adiabatic elastic constants, and $\alpha_{||}$ and α_{\perp} are the thermal expansivities parallel and perpendicular to the c axis. In the calculations of the γ 's between room temperature and 40°K they did not allow for the temperature variation of the elastic constants, which were not available then. A recalculation of their Grüneisen parameters, using our values for the temperature dependence of the elastic constants, shows that there is no significant change in $\gamma_{||}$, but that γ_{\perp} is reduced in absolute value. Table V lists the room-temperature γ 's and the values at 50°K, first those quoted by Bailey and Yates and then the recalculated ones using the low-temperature elastic constants.

The low-temperature Grüneisen parameters are of interest for comparison with theoretical calculations of anharmonic effects in graphite.^{12,13} It must be cautioned, however, that the value of γ_{\perp} at 50°K listed in Table V is subject to a large experimental error. Bailey and Yates quote an uncertainty in γ_{\perp} of about 23% at 40°K, due principally to the uncertainty in expansivity values. Moreover, γ_{\perp} depends strongly on C_{13} , which in our experiments is the least certain of the elastic constants.

B. Pressure

We can compare our high-pressure results with the results of previous measurements on CAPG and on pure single-crystalline graphite in several ways. Green *et al.*¹⁴ have recently reported high-pressure (to ~7 kbar) transit time measurements for modes 1 and 2 (longitudinal and shear modes propagating along the c axis) of CAPG. Using these data and certain appropriate approximations, these authors were able to determine the elastic constants C_{33} and C_{44} as a function of pressure and of

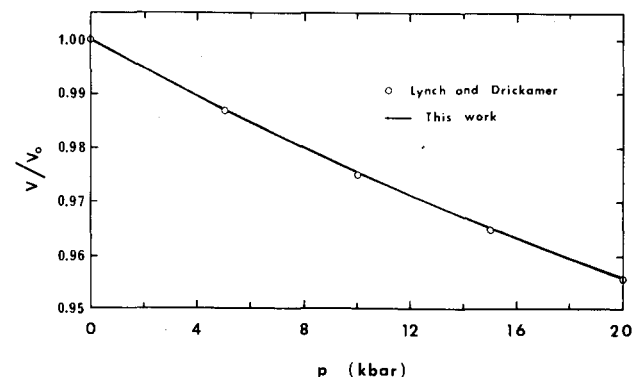


FIG. 5. Sample volume V as a function of pressure, normalized to volume V_0 at atmospheric pressure, calculated from the present ultrasonic measurements (solid line) and calculated from x-ray measurements of lattice parameters of Ceylon graphite due to Lynch and Drickamer (circles).

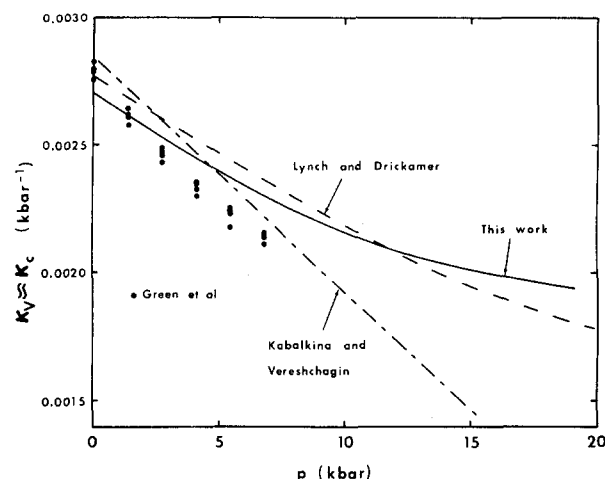


FIG. 6. Graphite c axis or volume compressibility as a function of pressure. The data of Green *et al.* were obtained on CAPG by ultrasonic techniques as were the data of this work. The results of Lynch and Drickamer and of Kabalkina and Vereshchagin were obtained on natural graphite crystals by x-ray measurements.

c -axis strain. They were also able to calculate the c -axis compressibility κ_c which is essentially equal to the volume compressibility κ_v . For the initial values of the elastic constant pressure derivatives Green *et al.* obtain $d\ln C_{33}/dp = (4.0 \pm 0.3) \times 10^{-2} \text{ kbar}^{-1}$ and $d\ln C_{44}/dp = (1.6 \pm 0.3) \times 10^{-2} \text{ kbar}^{-1}$. Our values are $d\ln C_{33}/dp = (2.6 \pm 0.3) \times 10^{-2} \text{ kbar}^{-1}$ and $d\ln C_{44}/dp = (0.80 \pm 0.12) \times 10^{-2} \text{ kbar}^{-1}$. Although there are great difficulties in measuring these derivatives and substantial uncertainties in the final results, it does appear that our pressure slopes are significantly smaller than those of Green *et al.*, and that the differences are outside the range of the experimental uncertainties. Although the source of the differences is not known, we will show below that our measurements are in good agreement with some x-ray compression measurements.

There have been several direct measurements of compression of natural graphite crystals. Piston displacement measurements were made by Bridgman,¹⁵ and high-pressure x-ray measurements have been made by Kabalkina and Vereshchagin¹⁶ and by Lynch and Drickamer.¹⁷ These measurements can be compared directly to the dimensional changes obtained in our self-consistent iterative data analysis scheme. (The differences between adiabatic and isothermal compressibilities are, again, ignored.) The data of Lynch and Drickamer are the most recent of the compression data, and the good agreement of our results with these data is shown in Fig. 5.

A somewhat more sensitive way to compare our data with the compression data is to compare the compressibilities as a function of pressure, in other words to compare the slopes of the compression curves to the ultrasonic compressibilities. (For this discussion the relations $\kappa_a \ll \kappa_c$ and $\kappa_c \approx \kappa_v$ should be kept in mind.) This comparison is shown in Fig. 6 for the two ultrasonic experiments done on CAPG and the two high-pressure x-ray experiments done on natural graphite crystals.

There are, of course, large uncertainties in obtaining slopes from compression curves, and there are also significant uncertainties in the ultrasonic data. Nevertheless, the values of the compressibilities obtained in the various experiments at atmospheric pressure agree to within experimental uncertainties. (The 1-atm value for the present experiment derives from the data of Blackslee *et al.*⁴) The variation of compressibility with pressure, however, falls into two distinct groupings: the ultrasonic data of Green *et al.* agree with the x-ray data of Kabalkina and Vereshchagin, while our ultrasonic results show better agreement with the x-ray data of Lynch and Drickamer.

The data of Kabalkina and Vereshchagin exhibit a large amount of scatter. The authors fit their data with a quadratic function of pressure, thereby assuming a constant slope for the compressibility-vs-pressure curve. It appears more realistic for this curve to exhibit a slope whose magnitude decreases at high pressure. In fact, with only a small change in the fit to the data, a compressibility-vs-pressure curve in substantially better agreement with the results of Lynch and Drickamer would be obtained.

In summary, the present compressibility results for CAPG are in reasonable agreement with the measurements of compressibility of natural graphite, lending support to the hypothesis that CAPG has bulk elastic properties very close to those of single-crystalline graphite.

ACKNOWLEDGMENTS

The authors thank Dr. A.W. Moore, Union Carbide Corporation, Parma Technical Center, Parma, Ohio, for supplying the CAPG samples; and Dr. R.W. Lynch, Sandia Laboratories, for making available some of the original data of Ref. 17.

*Work supported by the U.S. Atomic Energy Commission.

¹W.N. Reynolds, *Physical Properties of Graphite* (Elsevier, Amsterdam, 1968).

²See, e.g., H.M. Stoller, B.L. Butler, J.D. Theis, and M.L. Lieberman, in *Fiber Composites: State of the Art*, edited by J.W. Weeton and E. Scala (Metallurgical Society of AIME, New York, 1974).

³A.R. Ubbelohde, D.A. Young, and A.W. Moore, *Nature* (Lond.) **198**, 1192 (1963); *Proc. R. Soc. A* **280**, 153 (1964).

⁴O.L. Blackslee, D.G. Proctor, E.J. Seldin, G.B. Spence, and T. Weng, *J. Appl. Phys.* **41**, 3373 (1970).

⁵E.J. Seldin and C.W. Nezbeda, *J. Appl. Phys.* **41**, 3389 (1970).

⁶Fisher Scientific Co., Fair Lawn, N.J.

⁷H.J. McSkimin, *J. Acoust. Soc. Am.* **33**, 12 (1962).

⁸R.D. Peters, M.A. Breazeale, and V.K. Paré, *Phys. Rev. B* **1**, 3245 (1970).

⁹R.K. Cook, *J. Acoust. Soc. Am.* **29**, 445 (1957).

¹⁰I.J. Fritz, *J. Phys. Chem. Solids* **35**, 817 (1974).

¹¹A.C. Bailey and B. Yates, *J. Appl. Phys.* **41**, 5088 (1970).

¹²B.T. Kelly and P.L. Walker, Jr., *Carbon* **8**, 211 (1970).

¹³B.T. Kelly, *Carbon* **10**, 429 (1972).

¹⁴J.F. Green, P. Bolsaitis, and I.L. Spain, *J. Phys. Chem. Solids* **34**, 1927 (1973).

¹⁵P.W. Bridgman, *Proc. Am. Acad. Arts Sci.* **76**, 9 (1945); **76**, 55 (1948).

¹⁶S.S. Kabalkina and L.F. Vereshchagin, *Sov. Phys.-Dokl.* **5**, 373 (1960).

¹⁷R.W. Lynch and H.G. Drickamer, *J. Chem. Phys.* **44**, 181 (1966).